Shape Optimization for Reducing Stress at Ceramics/Metal Joints†

Hidekazu MURAKAWA* and Yukio UEDA**

Abstract

Due to the brittleness and poor machinability, ceramics is used in the form of composite structure with metals. However, stress concentration occurs at the region near the edge of interface between ceramics and metal. Such high stress may cause cracking of ceramics under thermal loads and reduce strength against external loads. In general, the stress concentration greatly depends on the geometry or the shape of the parts. The authors investigated the possibility of reducing stress concentration through controlling the shape of joint. For this purpose, the problem is treated as an optimization problem and a shape optimization procedure is proposed. Further, it is applied to simple example problems, which can be considered as linear thermal-elastic problems, to show that the proposed optimization technique can be an useful tool to design shapes of joints between dissimilar materials.

KEY WORDS : (Shape Optimization) (Optimum Design) (Ceramics) (Metal) (Joint) (Thermal Stress) (Finite Element Method) (Allowable Stress)

1. Introduction

New-Ceramics has a great potential in various engineering applications because of its superiority in resistance to high temperature and corrosion and its unique physical or electronical functions. However, most ceramics is brittle and poor in machinability. These drawbacks are overcome by introducing composite structure consisting of ceramics and metal, which has ductility and good machinability. To integrate the two materials to construct a composite structure, the bonding technique plays a crucial role. In most cases, ceramics and metal are joined at elevated temperature, such as brazing and diffusion bonding. Due to the large difference in thermal expansion coefficients of two materials, significant magnitude of residual stress is produced during the cooling process after joining. Such residual stress created at the bonding region may cause cracking or reduce the bonding strength. Thus, it is desirable to minimize the size of the residual stress and various techniques are developed for this purpose. One of such techniques is to introduce the interlayer. The effects of the thickness and the mechanical properties of the interlayer on the reduction of the residual stress have been investigated by T. Terasaki et al.[1),2)] and others[3)]. Another possible technique is reducing stress through controlling the shape of the bonding zone[4)]. Both the proper selection of the interlayer and control of shape are optimum design problems in their nature. However, reports in which the problems are dealt as optimum design problem are hardly found.

In this report, the authors treated the problem of reducing the residual stress through shape control as an optimum design problem and developed a numerical method to automatically determine the optimum shape for the given conditins. The formulation of the problem and the outline of the optimization procedure are shown in Chapter 2. Further, typical examples of optimization, which can be idealized as thermal-elastic problems, are presented in Chapter 3.

2. Optimization Method

2.1 Representation of shape and its modification

Two dimensional shape optimization problem, as shown in **Fig. 1**, is considered. In this report, both ceramics and metal parts are assumed to be cylindrical and joined coaxially, so that the problem can be treated as axisymmetric thermal-elastic problems. The shapes of ceramics and metal are represented by the lines in r-z plane which correspond to surfaces and interface of the materials.

On the other hand, the domain for the analysis is subdivided into finite number of elements (3 node triangular elements are used in this report) and nodes are defined at the corners of the elements. Since the nodes are also defined on the surface and the interface, the shape of the joint can be represented by their coordinates. Further, the modification of the shape can be

† Received on October 31, 1989
* Associate Professor
** Professor

Transactions of JWRI is published by Welding Research Institute of Osaka University, Ibaraki, Osaka 567, Japan

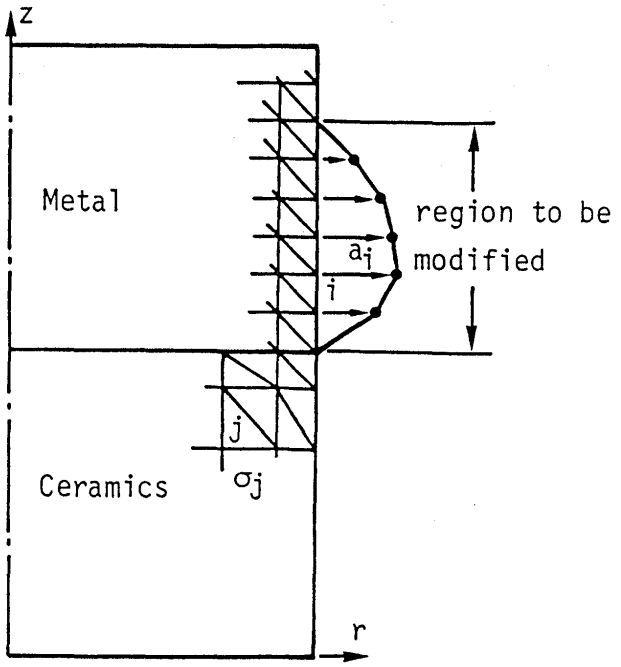

Fig. 1 Description of shape and its modification.

achieved by moving the nodes lying on the surface or the interface. If the part of the boundary to be modified and the direction in which the nodes can move are a priori given, the modified shape can be uniquely defined by the distance of move a_i of the i-th node. In other words, the shape can be defined by a_i as design parameters.

In general, the change of the shape by optimization is fairly large. The elements near modified boundary may be excessively distorted if only the nodes on boundary are moved. To prevent the loss of accuracy, it is necessary to regenerate the finite element mesh with the movements of boundary nodes[5]. If only mesh distortion is concerned, Boundary Element Method (BEM), in which no internal nodes or elements are defined, is suitable for shape optimization[6),7)]. But, if the problem becomes nonlinear, such as the thermal-elastic-plastic problem, the Finite Element Method (FEM) seems to be superior to BEM. Thus, FEM is employed as a simulation tool in the present study.

2.2 Condition of optimization

The optimum shape is defined by the following two conditions.

(1) *state of stress*

Maximum principal stress σ_j at the evaluation point j (element j in case of FEM using 3 node triangular element) are monitored. The shape is modified so that σ_j becomes less than or equal to the objective allowable stress σ_0 or the value exceeding σ_0 is minimized when σ_j remains greater than σ_0.

(2) *arc length of the boundary to be modified*

In case of practical engineering problems, there are certain restrictions so that the product can be machined or produced and fulfill the required function. The shape is also subjected to various constraints. As one of the constraint, the arc length is assumed to be constant and optimum shape is searched under this condition. In other words, when the original arc length is L_0, the arc length of the optimum shape is kept αL_0, where α is a given constant and referred to as arc length factor.

2.3 Objective function

The optimization problem described in the preceding section can be formulated as a least square type optimization problem. If the value of stress exceeding the objective allowable stress, i.e. $w_j = (\sigma_j - \sigma_0)$, is large, the corresponding shape is considered to be inferior. Hence, the magnitude of excess w_j can be considered as a local measure of the poorness of the shape. Further, their weighted sum W can be used as an objective function or a global measure, such that

$$W = \sum A_j w_j^2 \tag{1}$$

where, A_j are proper weights and

$$w_j = \sigma_j - \sigma_0 \quad \text{if} \quad \sigma_j > \sigma_0$$
$$w_j = 0 \quad \text{if} \quad \sigma_j \leqq \sigma_0$$

On the other hand, the coordinates of the boundary nodes on the modified boundary must satisfy the constraint on the arc length. However, this condition is nonlinear and it is difficult to satisfy it a priori. To overcome this difficulty, the optimization problem is modified to that without subsidiary condition.

2.4 Optimization problem without subsidiary condition

By introducing Lagrange's multiplier λ, the subsidiary condition can be embedded in the objective function and new objective function W^* in the following form is derived.

$$W^*(a_i, \lambda) = \sum_j A_j \{w_j(a_i)\}^2 - \lambda[\sum_k \{(x_{k+1} - x_k)^2 + (y_{k+1} - y_k)^2\}^{1/2} - \alpha L_0] \tag{2}$$

where, (x_k, y_k) are coordinates of the node on modified boundary. It should be noted that the variables a_i or λ are not subjected to any subsidiary condition and the optimum shape can be obtained through the stationarity condition of the objective function W^*.

If the boundary to be modified is the side surface of the metal which is parallel to z axis as shown in Fig. 1 and the nodes on the boundary can move in r direction, the objective function W^* can be given as,

$$W^*(a_i, \lambda) = \sum_j A_j|w_j(a_i)|^2 - \lambda[\sum_k\{(x^0_{k+1}+a_{k+1}-x^0_k-a_k)^2 + (y^0_{k+1}-y^0_k)^2\}^{1/2} - \alpha L_0] \quad (3)$$

where

a_k :distance of move

$\sum_j$:summation over the elements in the region to be monitored

$\sum_i$:summation over the nodes on the boundary to be modified

(x^0_k, y^0_k) :coordinates of the k-th node in the original shape

2.5 Iterative procedure

The objective function given by Eq. (3) is a highly nonlinear function of a_i and λ. Thus, the stationarity condition, i.e.

$$\partial W^*/\partial a_i = 0, \ \partial W^*/\partial \lambda = 0 \quad (4)$$

become nonlinear and the solution can not be found in single step. Therefore, iterative solution procedure is employed. Let Δa_i and $\Delta\lambda$ be the corrections to the approximate values found in the n-th step, a_i^n and λ^n, the new approximation can be given as,

$$a_i^{n+1} = a_i^n + \Delta a_i, \ \lambda^{n+1} = \lambda^n + \Delta\lambda \quad (5)$$

On the other hand, if the objective function W^* is expanded in Taylor series and the terms higher than the second order in Δa_i and $\Delta\lambda$ are neglected, the objective function W^* can be reduced to,

$$W^*(\Delta a_i, \Delta\lambda) = W_0^*(a_i^n, \lambda^n) + W_1^*(\Delta a_i, \Delta\lambda) + W_2^*(\Delta a_i, \Delta\lambda) \quad (6)$$

where W_0^*, W_1^* and W_2^* are constant, linear and second order terms in Δa_i and $\Delta\lambda$ which are defined as,

$$W_0^* = \sum A_j|w_j(a_i^n)|^2 - \lambda^n[L^n - \alpha L_0] \quad (7)$$

$$W_1^* = 2\sum A_j w_j(a_i^n)\frac{\partial w_j}{\partial a_k}\Delta a_k - \Delta\lambda[L^n - \alpha L_0] - 2\lambda^n L^{-1}\sum(x^0_{k+1}-x^0_k+a_{k+1}-a_k)(\Delta a_{k+1}-\Delta a_k) = -\begin{Bmatrix}\Delta a_i\\ \Delta\lambda\end{Bmatrix}^T\begin{Bmatrix}F_a\\ F_b\end{Bmatrix} \quad (8)$$

$$W_2^* = \sum A_j\frac{\partial w_j}{\partial a_i}\frac{\partial w_j}{\partial a_k}\Delta a_i\Delta a_k - 2L^{-1}\sum(x^0_{k+1}-x^0_k+a_{k+1}-a_k)\Delta\lambda(\Delta a_{k+1}-\Delta a_k) - 1/2\lambda^n L^{-3}\sum(y^0_{k+1}-y^0_k)^2(\Delta a_{k+1}-\Delta a_k)^2 = \frac{1}{2}\begin{Bmatrix}\Delta a_i\\ \Delta\lambda\end{Bmatrix}^T\begin{vmatrix}K_{aa} & K_{ab}\\ K_{ba} & K_{bb}\end{vmatrix}\begin{Bmatrix}\Delta a_k\\ \Delta\lambda\end{Bmatrix} \quad (9)$$

Also, the arc length L^n, at the n-th step, is given by,

$$L^n = \sum\{(x^0_{k+1}-x^0_k+a_{k+1}-a_k)^2+(y^0_{k+1}-y^0_k)^2\}^{1/2}$$

The objective function W^* given by Eq. (6) can be rewritten in a matrix form, such that,

$$W^*(\Delta a_i, \Delta\lambda) = W_0^*(a_i^n, \lambda^n) - \begin{Bmatrix}\Delta a_i\\ \Delta\lambda\end{Bmatrix}^T\begin{Bmatrix}F_a\\ F_b\end{Bmatrix} + \frac{1}{2}\begin{Bmatrix}\Delta a_i\\ \Delta\lambda\end{Bmatrix}^T\begin{vmatrix}K_{aa} & K_{ab}\\ K_{ba} & K_{bb}\end{vmatrix}\begin{Bmatrix}\Delta a_k\\ \Delta\lambda\end{Bmatrix} \quad (10)$$

Further, applying the following stationarity condition,

$$\partial W^*/\partial\Delta a_i = 0, \ \partial W^*/\partial\Delta\lambda = 0 \quad (11)$$

a set of linear algebraic equations in terms of Δa_i and $\Delta\lambda$ are derived, such that

$$\begin{vmatrix}K_{aa} & K_{ab}\\ K_{ba} & K_{bb}\end{vmatrix}\begin{Bmatrix}\Delta a_i\\ \Delta\lambda\end{Bmatrix} = \begin{Bmatrix}F_a\\ F_b\end{Bmatrix} \quad (12)$$

Solving Eq. (12), the correction values Δa_i and $\Delta\lambda$ are obtained and the new approximate values are given by Eq. (5). This procedure is repeated until the convergence is attained and the optimum shape for the given arc length αL_0 is obtained.

2.6 Optimality of the solution

The formulation and the optimization procedure is shown in the preceding section. In this section, the optimality of the solution is examined.

In general, optimum solution is the solution which minimizes the objective function among the all possible alternatives which satisfy the given constraint conditions. Thus, for the optimality in the strict sense, the objective function must be defined in such a way that any subjective or ambiguous element is excluded. Also, the solution must be searched among the all possible alternatives.

Concerning these two requirements, the solucion obtained by the proposed method can bot be an optimum solution in the strict sense. One reason may be found in the fact that the evaluation of the stress state involves objective allowable stress σ_0 and weight A_j, which are given relatively arbitraryly. The variation of these values may cause change in optimum shapes. As for the search area, the boundary to be modified and its arc length are a priori given. This implies that the obtained solution is a local optimum within the above conditions.

However, the proposed method can be regarded as one of the tools for practical design. Though the criteria

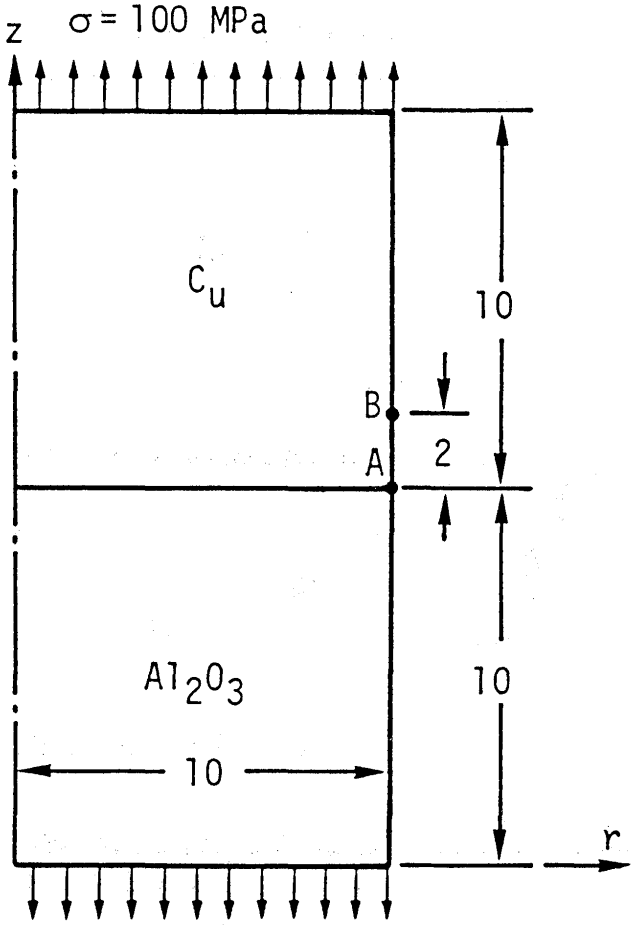

Fig. 2 Example model and region to be modified.

Table 1 Mechanical properties of materials

	Al_2O_3	Cu
Young's modulus (GPa)	370	130
Poisson's ratio	0.25	0.3
Thermal expansion coef. (1/K)	$7.9X10^{-6}$	$17.7X10^{-6}$

for the crack initiation is not clearly understood yet, if it is assumed that the crack initiates when the maximum tensile stress reaches the given critical stress, it is necessary to reduce the magnitude of the stress below the critical value. In such a case, the proposed method based on the objective allowable stress is quite suitable for this purpose. On the other hand, it may be desirable to control the shape of metal rather than ceramics due to machinability. It is also desirable to limit the degree of shape modification in order to ensure the designed function of the product. Thus, the idea of prescribing the boundary to be modified and its arc length is also practical.

In the case when the optimum shape close to the optimum in the strict and global sense is required, the

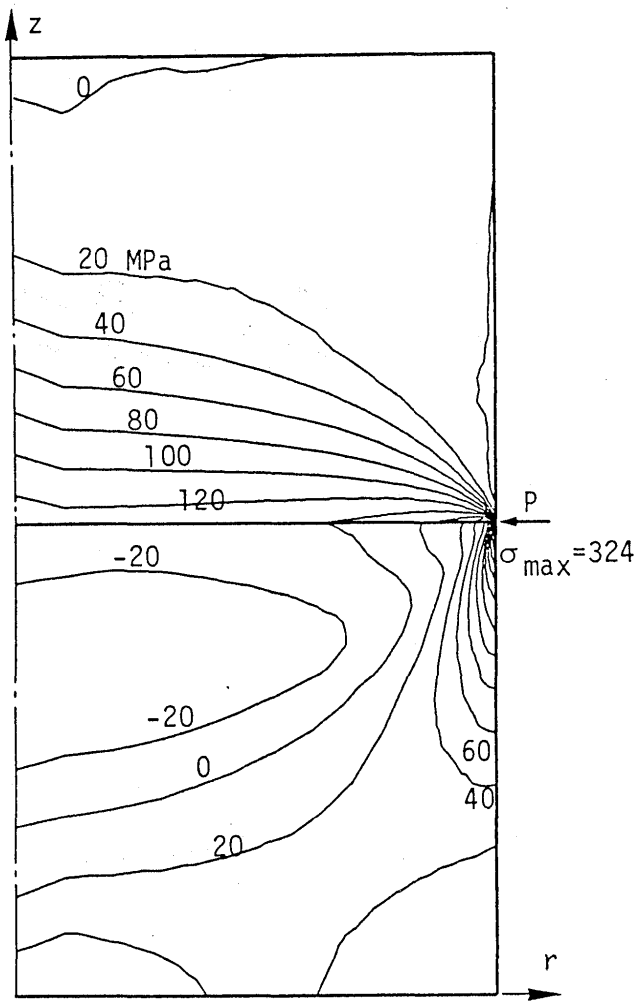

Fig. 3 Distribution of the largest principal stress in the original model under thermal load.

solution must be searched with changing the boundary to be modified and its arc length. The optimization process and the optimum shapes are shown for simple examples in the next chapter. Especially, the effects of the prescribed constraining conditions and loading conditions on the optimum shape are discussed.

3. Example of Shape Optimization

3.1 Example model

The model for the example problem is shown in **Fig. 2**. It consists of ceramics (Al_2O_3) and metal (Cu) parts with the same size. Their height and the diameter are 10 mm and 20 mm, respectively. It is assumed that the variations of material constants with temperature can be neglected and the values at room temperature are used. **Table 1** shows the Young's moduli, Poison's ratios and thermal expansion coefficients for the two materials.

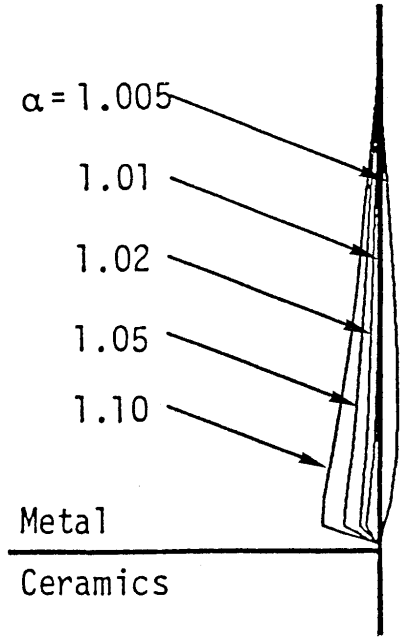

Fig. 4 Optimum shapes obtained for the case under thermal load.

3.2 Condition of optimization

The shapes are optimized under the conditions which are given as the combination of the following loading conditions and constraints.

loading condition

(1) thermal stress due to temperature drop by 100°C
(2) uniform stress of 100 MPa is acting in z direction as an external load
(3) the two loads described by (1) and (2) are acting simultaneously.

boundary to be modified

The side surface A-B of the metal, the length of which is 2 mm, is modified under five different arc length, i.e.

$$L = 1.005L_0,\ 1.01L_0,\ 1.02L_0,\ 1.05L_0,\ 1.10L_0$$

In the present problem, it is assumed that crack occurs only in the ceramics and stress state is monitored only in the ceramics. Hence, the first term in the right hand side of Eq. (2) becomes the summation over the elements in the ceramics part. On the other hand, the weight A_j involved in the objective function is assumed to be 1.0 for simplicity.

3.3 Procedure of optimization

The procedure of the optimization is shown using the problem under the thermal load as an example. The distribution of the largest principal stress in the original shape is shown in **Fig. 3**. The maximum value of the stress occurs at point P, which is at the edge of the interface, and its value σ_{max} is 324.5 MPa. The shape is optimized by setting the objective allowable stress as 50% of σ_{max}. In general, certain type of singularity is expected at the edge of the interface. However, the effect of such singularity may not be fully counted in the present method which uses discrete approximation by FEM.

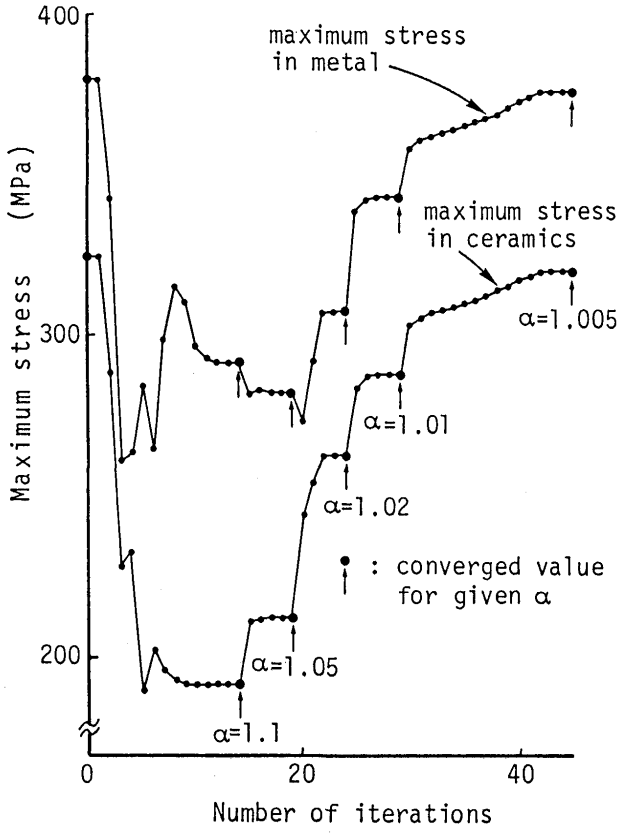

Fig. 5 Changes of maximum tensile stress in ceramics and metal during iteration process.

As discussed in the preceding chapter, the optimum shape is searched through an iterative procedure based on the linearization of the objective function. It is necessary to give a set of proper initial values. The following values are used as initial values for the case in which $\alpha = 1.10$.

$$a_i = 0,\ \lambda = 10^4$$

Once the solution for $\alpha = 1.10$ is obtained, it is used as an initial value to get the solution for $\alpha = 1.05$. The solutions for the remaining values of arc length factor can be determined successively.

The optimum shapes for the five different values of α are shown in **Fig. 4**. The process of the iterative procedure is described by **Fig. 5**, which shows the variation of the maximum stress in both ceramics and metal with the iteration steps. As seen from Fig. 5, 14 steps are required to get the convergence for the first case with $\alpha = 1.10$. Only 5 or 6 iterations are necessary for the

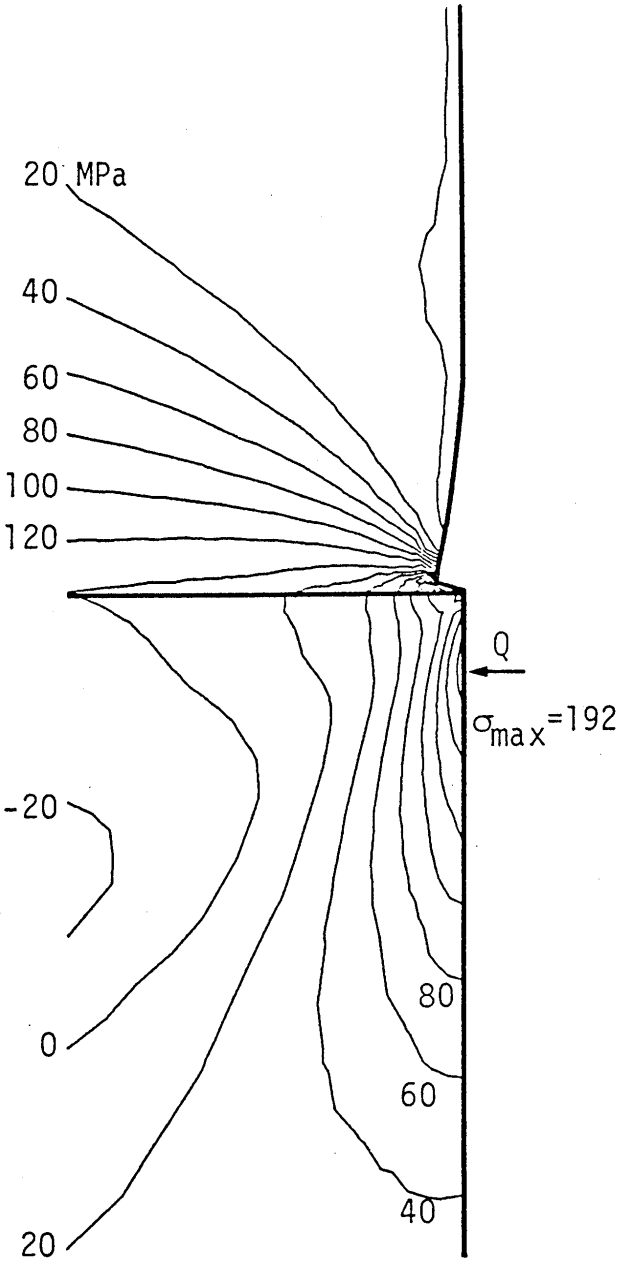

Fig. 6 Distribution of the largest principal stress in the model with optimum shape under thermal load (α =1.10).

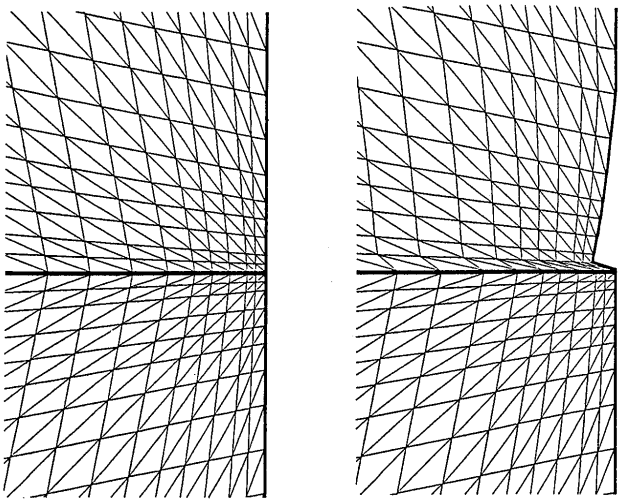

Fig. 7 Mesh divisions for original and optimum shapes (α = 1.10).

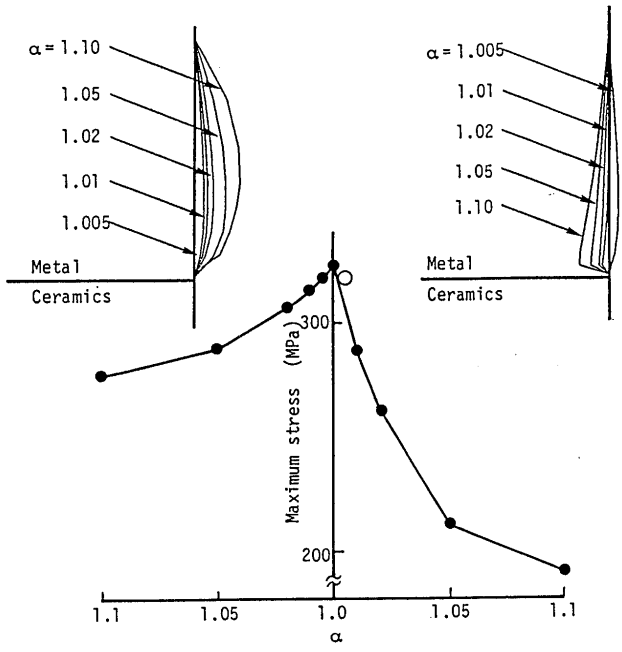

Fig. 8 Comparison of two possible types of shapes effective to reduce residual stress.

convergence in the successive cases with $\alpha = 1.05$, 1.02, 1.01. However, large number of iterations are required when $\alpha = 1.005$ because of the change of the mode of shape from concave to convex form. The distribution of the maximum principal stress for the optimum shape with $\alpha = 1.10$ is shown in **Fig. 6**. Comparing Figs. 3 and 6, the optimum shape has an undercut type form and the point where the maximum stress occurs shifts about 0.8 mm downwords in the ceramic part from the interface. The value of stress itself is reduced by 40% compared to that in the original shape. The reduction ratio of the stress in ceramics increases with the depth of the undercut, in other words the value of α, as shown by Fig. 5. The maximum stress in the metal also shows the same tendency and decreases with α. As mentioned earlier, the finite element mesh is automatically redefined at every step of optimization. The finite element meshes near the interface in original and optimum ($\alpha = 1.10$) shapes are compared in **Fig. 7**. Though, the automatic remeshing is employed, the element near the edge of the interface is largely distorted. Thus, the expected accuracy of the stress analysis in this case may be poor compared to other cases with small value of α.

In case of this example, the initial value of λ is assumed to be positive number, namely $\lambda = 10^4$, and optimization is started from $\alpha = 1.10$. If negative value,

such as -10^4, is used as an initial value of λ and the optimization is started from $\alpha = 1.005$ toward large value of α, the convex forms are obtained as optimum shapes as shown in **Fig. 8**. It should be noted that the stress can be reduced by both concave and convex forms when only thermal stress is considered.

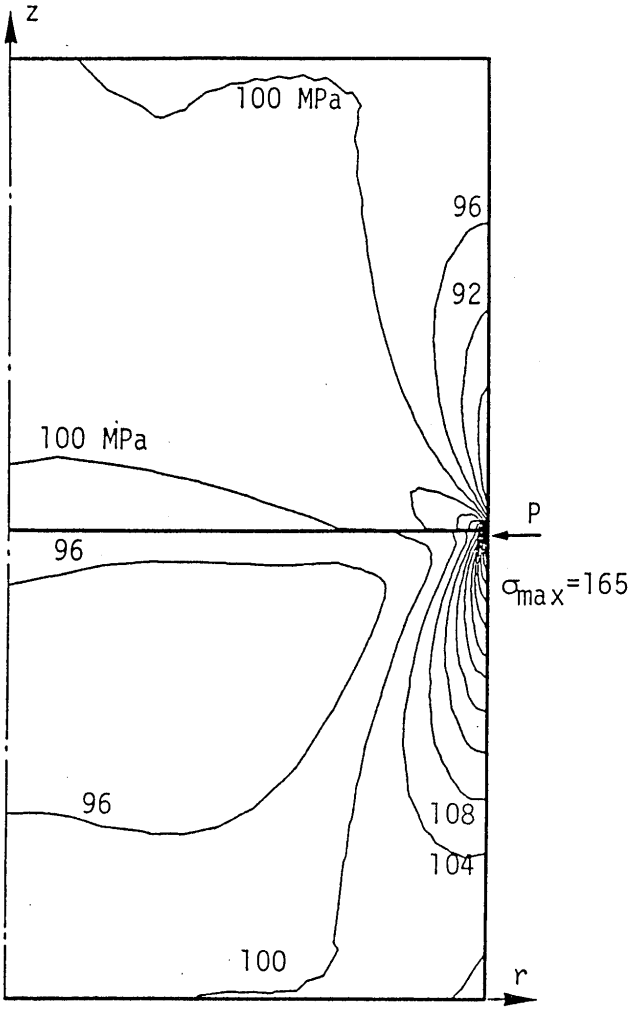

Fig. 9 Distribution of the largest principal stress in the original model under external load.

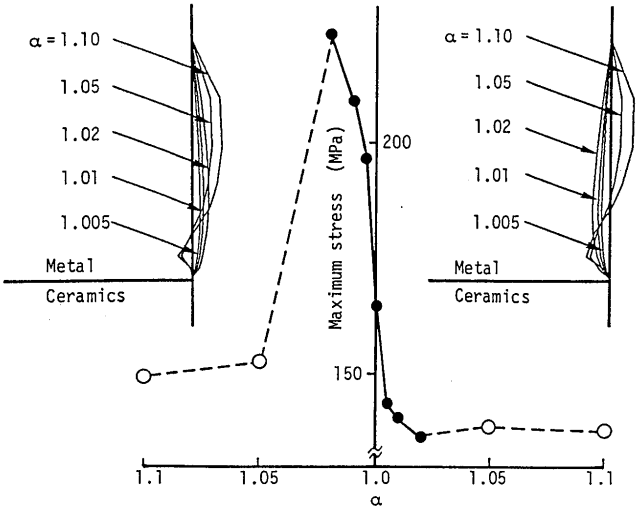

Fig. 10 Optimum shapes and the maximum stresses in ceramics under external load.

3.4 Loading condition and optimum shape

It is found that both concave and convex form is

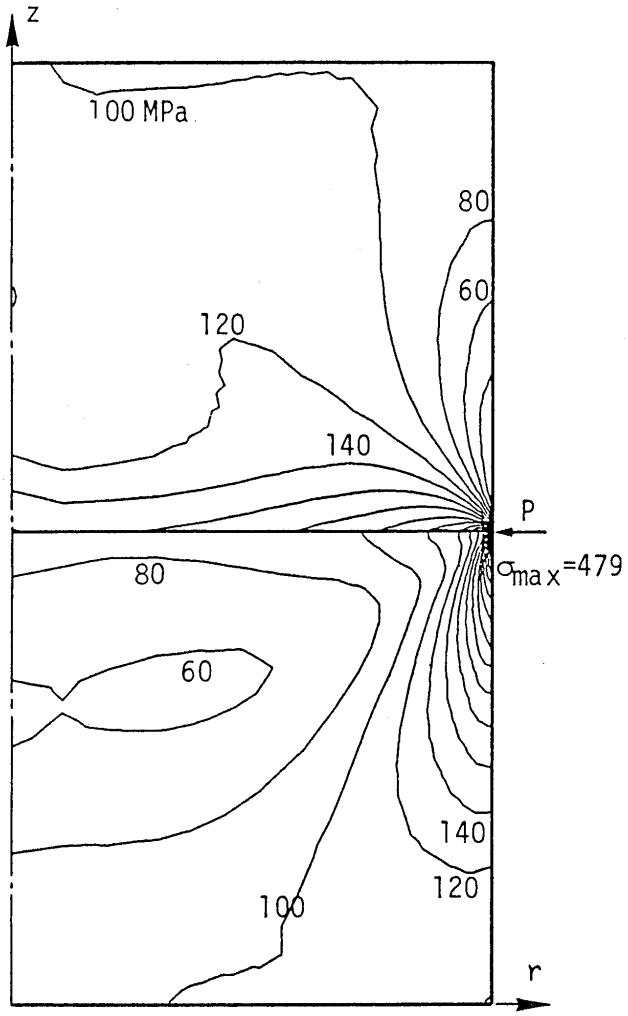

Fig. 11 Distribution of the largest principal stress in the original model under combination of thermal and external loads.

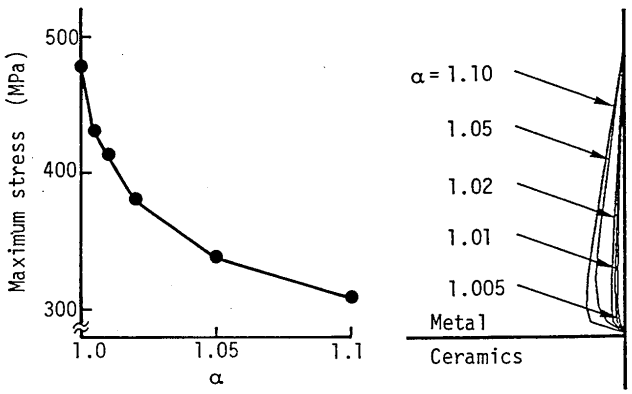

Fig. 12 Optimum shapes and the maximum stresses in ceramics under combined loads.

effective to reduce the stress when only thermal load is acting. However, external loads, such as the centrifugal force, may act on the ceramics/metal joint in practical situation. Hence, the optimum shapes under external load alone and combination of thermal and external loads are computed. By comparing the results of optimization, the effect of the loading condition on the optimum shape is examined in this section.

Figure 9 shows the stress distribution in the original shape under the external load alone. The external load is acting uniformly in z direction and its magnitude is assumed to be 100 MPa. The maximum stress occurs at point P and its value σ_{max} is 164.8 MPa. The shape is optimized with setting the objective allowable stress σ_0 as 75% of the maximum stress σ_{max}. The maximum stresses in the ceramics are plotted against arc length factor α in **Fig. 10**. The convex forms are obtained when a positive value is chosen as the initial value of λ. On the contrary, if initial value of λ is negative, concave shapes are obtained. The stable converged solutions are obtained only for small values of α and those for large α, denoted by open circles in Fig. 10, are rather unstable.

In contrast to the case under thermal stress, The stress in the optimum shape rapidly increases with α if the shape is convex. Thus, only concave form is effective to reduce the stress in the case where external load is acting.

Similarly, the shape is optimized for the case in which both thermal and external loads are acting. The stress distribution in the original shape is shown in **Fig. 11**. The maximum stress σ_{max} in this case is 479.2 MPa. The objective allowable stress is chosen to be 50% of σ_{max}. In this case, only concave shape is obtained as stable optimum shapes as shown by **Fig. 12**. The reduction ratio of the stress becomes approximately 35% when $\alpha = 1.10$.

4. Conclusion

A shape optimization technique is proposed as one of the method to reduce the stress at the ceramics/metal joints. The mathematical formulation and the optimization procedure are presented in this report. Further, it is shown through numerical examples that the proposed technique can be a promissing tool for the design of the joints between dissimilar materials.

However, the fracture criteria for ceramics, the singularity in stress distribution at the edge of interface and the effect of nonlinearity such as plastic deformation of metal have not been discussed in the present report. These will be taken as the next research subjects.

References

1) T. Terasaki, K. Seo and T. Hirai, "Dominating Parameters of Residual Stress Distribution -Residual Stress in Bonded Dissimilar Materials, Part 1-", Quarterly Journal of the Japan Welding Soceity, Vol.5, No.4 (1987 in Japanese), 533-537.
2) T. Terasaki, T. Hirai and K. Seo, "Effect of Mechanical Constant and Specimen Size on Residual Stress -Residual Stress in Bonded Dissimilar Materials (Part II)-", Quarterly Journal of the Japan Welding Society, Vol.6, No.2 (1988 in Japanese), 284-288.
3) K. Seo, M. Kusaka, F. Nogata, T. Terasaki, Y. Nakao and K. Saida, "Study on the Thermal Stress at Ceramics-Metal Joint", Trans. of Japan Society of Mechanical Engineers Series A, Vol.55, No.510 (1989 in Japanese), 312-317.
4) H. Koguchi, T. Kaya, Y. Ohtani and T. Yada, "Reliability Evaluation of Joints of Ceramics and Metal", Trans. of Japan Society of Mechanical Engineers Series A, Vol.55, No.513 (1989 in Japanese), 1121-1125.
5) N. Kikuchi, K. Y. Chung, T. Torigaki and J. E. Taylor, "Adaptive Finite Element Methods for Shape Optimization of Linearly Elastic Structures", Computer Methods in Applied Mechanics and Engineering, Vol.57 (1986), 67-89.
6) H. Murakawa, T. Myojin, S. Tokumasu and T. Aso, "Geometry Optimization to Reduce Stress Concentration Using Boundary Element Method", Trans. of Japan Society of Mechanical Engineers Series A, Vol.49, No.439 (1984 in Japanese), 396-402.
7) S. Tokumasu, H. Murakawa and T. Myojin, "Geometry Optimization of Electrode by Boundary Element Method", Trans. of the Society of Electrical Engineers of Japan Series B, Vol.104, No.4 (1984 in Japanese), 53-61.